Electronic Supplementary Material (ESI) for Journal of Materials Chemistry A.
This journal is © The Royal Society of Chemistry 2017

Supporting Information

Hollow FeNi-based hybrid polyhedron derived from unique sulfur-modulating coordinated transition bimetal complexes for efficient oxygen evolution reaction

Hongyan Qiao, Jiaxi Yong, Xiaoping Dai*, Xin Zhang, Yangde Ma, Mengzhao Liu, Xuebin Luan, Jianchang Cai, Yang Yang, Huihui Zhao and Xingliang Huang

State Key Laboratory of Heavy Oil Processing, China University of Petroleum, Beijing 102249, China

*E–mail: daixp@cup.edu.cn

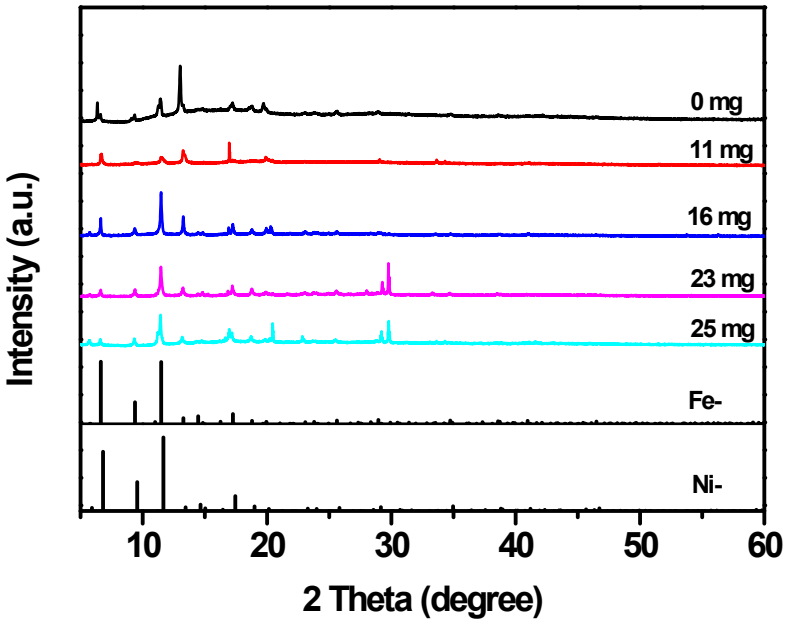

Fig. S1 XRD patterns of (A) *x*-S@FeNi-coordinated precursors with different amounts of sulfur (*x*= 0, 11, 16, 23, 25 mg), and Fe-, Ni-precursors without sulfur.

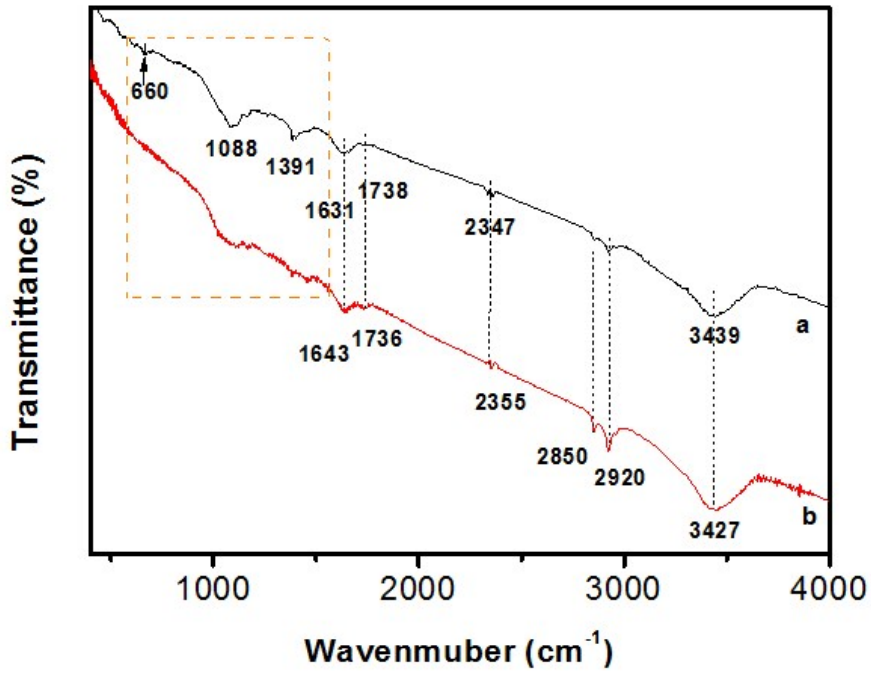

Fig. S2 FTIR spectra of (A) 23-S@FeNi-coordinated precursor, (B) FeNi-coordinated precursor with the addition of sulfur.

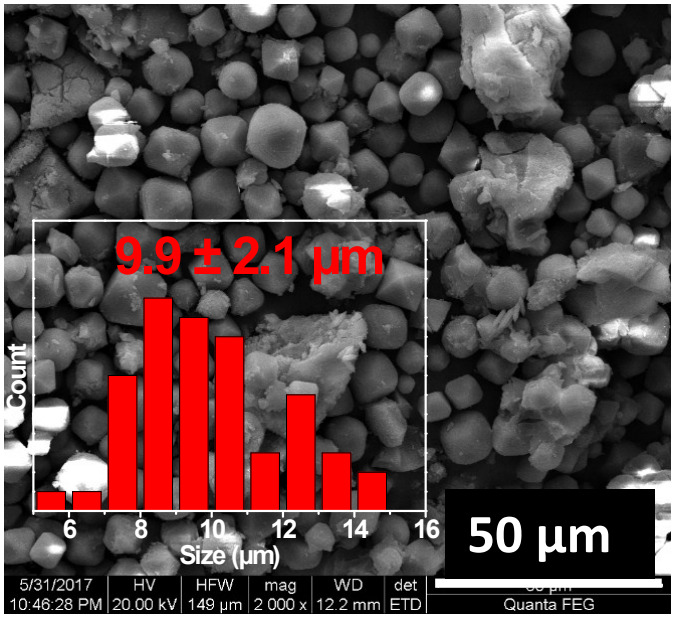

Fig. 3 SEM images of morphological evolution of 23-S@FeNi-coordinated precursor with various solvothermal time of 5 h.

Table S1. Elemental analyses of S in *x*-S@FeNi-coordinated precursors

x-S@FeNi-coordinated precursors	Amount of S
11	1.92
16	2.78
23	3.85
25	4.27

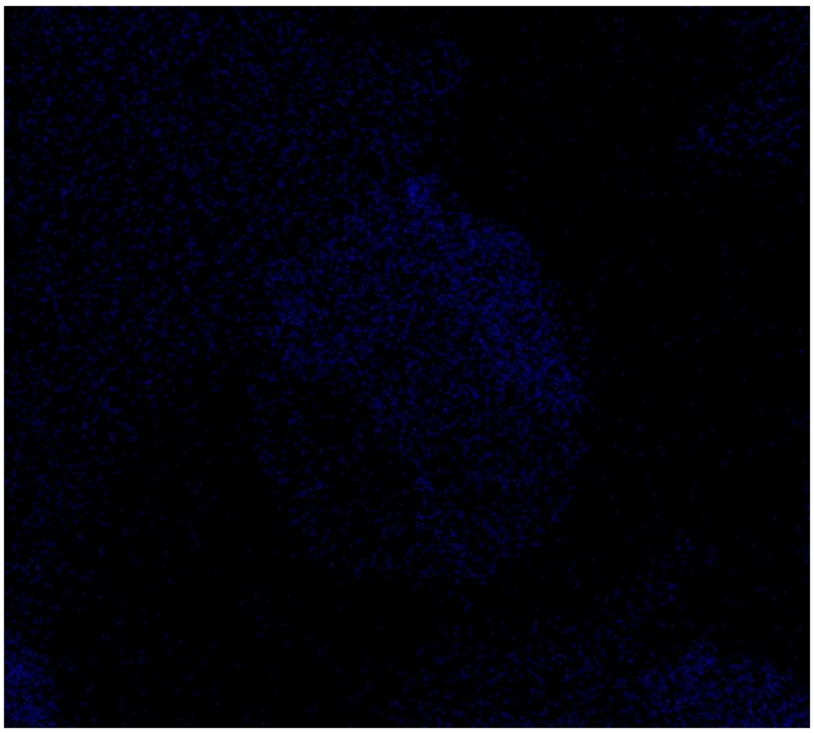

Fig. S4 Elements mapping of O in 23-S-FeNi@NC-3

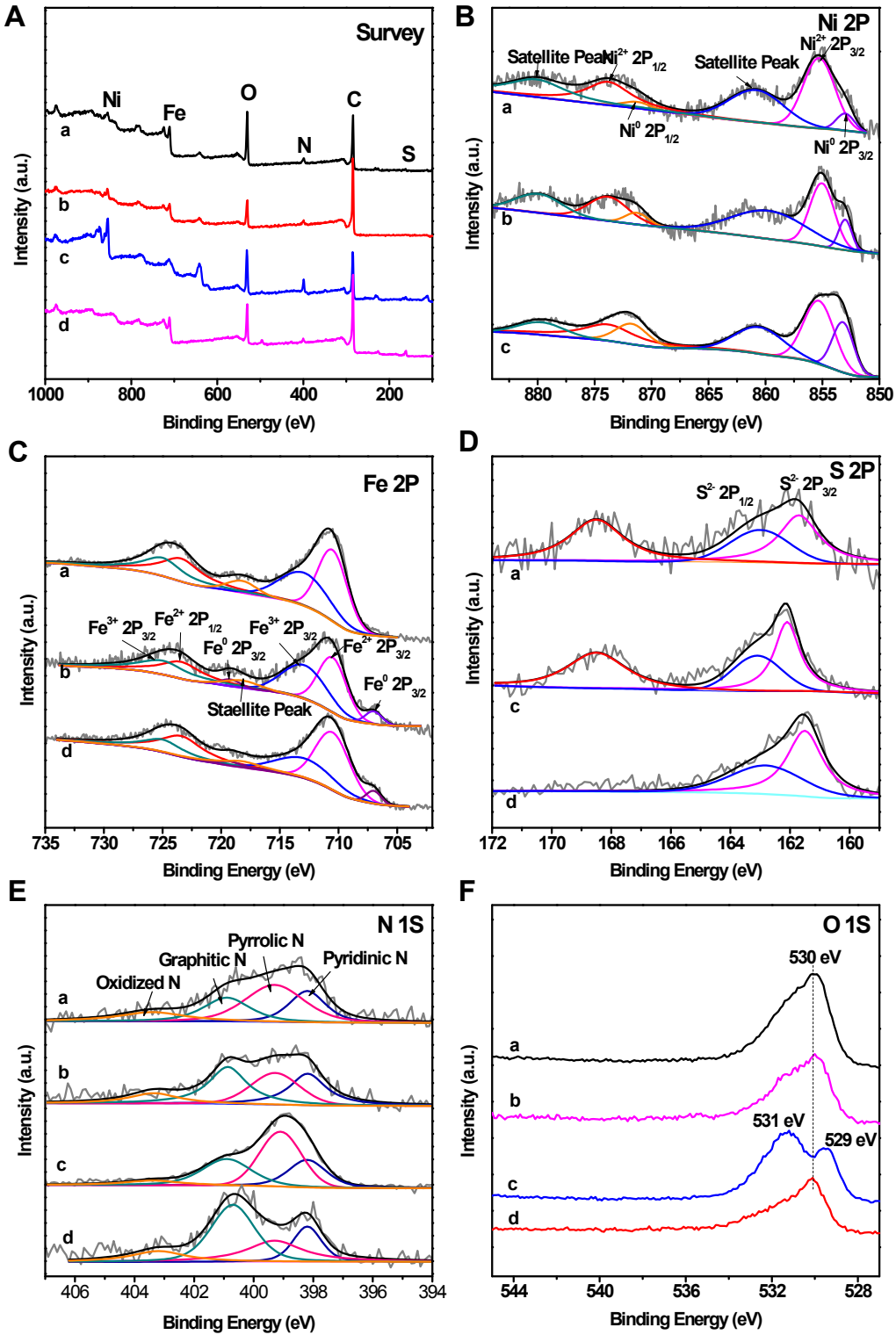

Fig. S5 (A) XPS survey spectra, and high–resolution scans of (B) Ni2p, (C) Fe 2p, (D) S 2s, (E) N 1s, (F) O 1s for (a) 23-S-FeNi@NC-3, (b) FeNi@NC-3, (c) 23-S-Ni@NC-3 and (d) 23-S-Fe@NC-3.

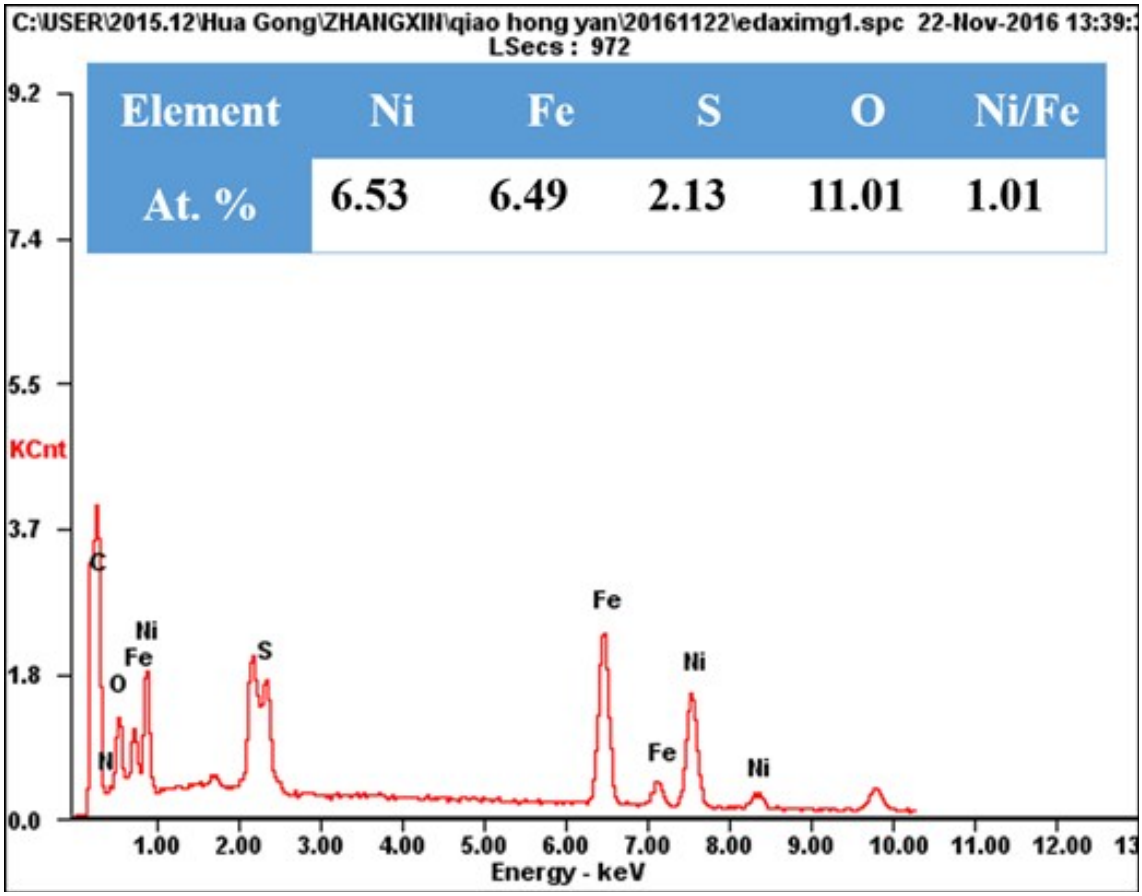

Fig. S6 EDS of 23-S-FeNi@NC-3.

Table S2. Composition, BET surface area and pore size of the FeNi-based composites

Catalysts	TXRF (wt.%)			XPS (at.%)				BET	Pore size
	Fe	Ni	S	Fe	Ni	S	N	$m^2 g^{-1}$	nm
23-S-FeNi@NC-3	28.1	29.1	4.4	8.97	2.64	2.15	4.52	159.3	4.02
FeNi@NC-3	31.8	28.1	0	5.21	2.94	0	4.07	136.1	3.83
23-S-Ni@NC-3	42.5	0	1.9	0	12.4	2.82	4.25	268.9	3.82
23-S-Fe@NC-3	0	47.0	3.3	7.46	0	2.68	2.82	24.4	3.86

Table S3. The N-doping content and types of nitrogen from XPS

Catalysts	N content (at. %)	Pyridinic N	Pyrrolic N	Graphic N	Oxidized N
23-S-FeNi@NC-3	4.52	22.5	39.9	22.7	14.9
FeNi@NC-3	4.07	27.4	26.9	33.4	12.3
23-S-Ni@NC-3	4.25	22.8	42.1	28.1	7.0
23-S-Fe@NC-3	2.82	17.8	26.0	43.0	13.3

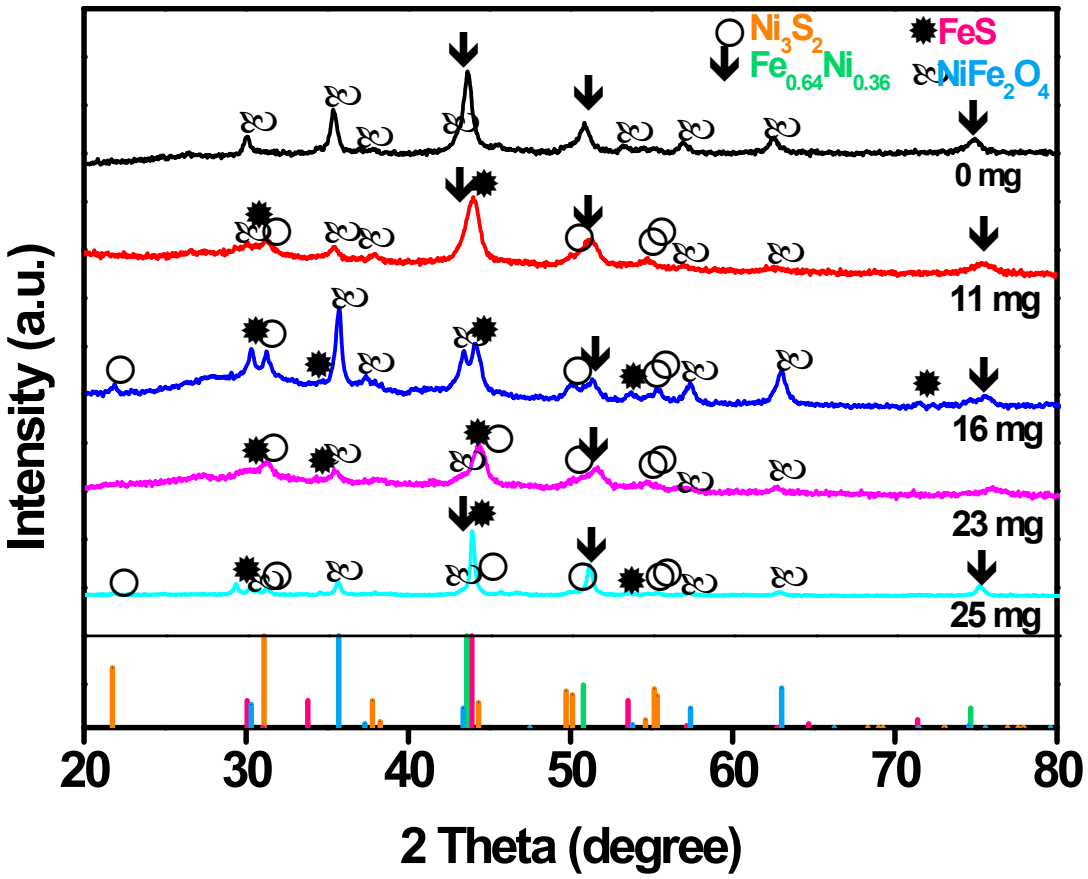

Fig. S7 XRD patterns *x*-S-FeNi@NC-3 with different amounts of sulfur (*x*=0, 11, 16, 23, and 25 mg). The vertical lines in orange, red, green and blue are the simulated diffraction peak positions of Ni_3S_2 (JCPDS card no. 44-1418), FeS (JCPDS card no. 01-1247), $Fe_{0.64}Ni_{0.36}$ alloys (JCPDS card no. 47-1405) and $NiFe_2O_4$ oxides (JCPDS card no. 54-0964), respectively.

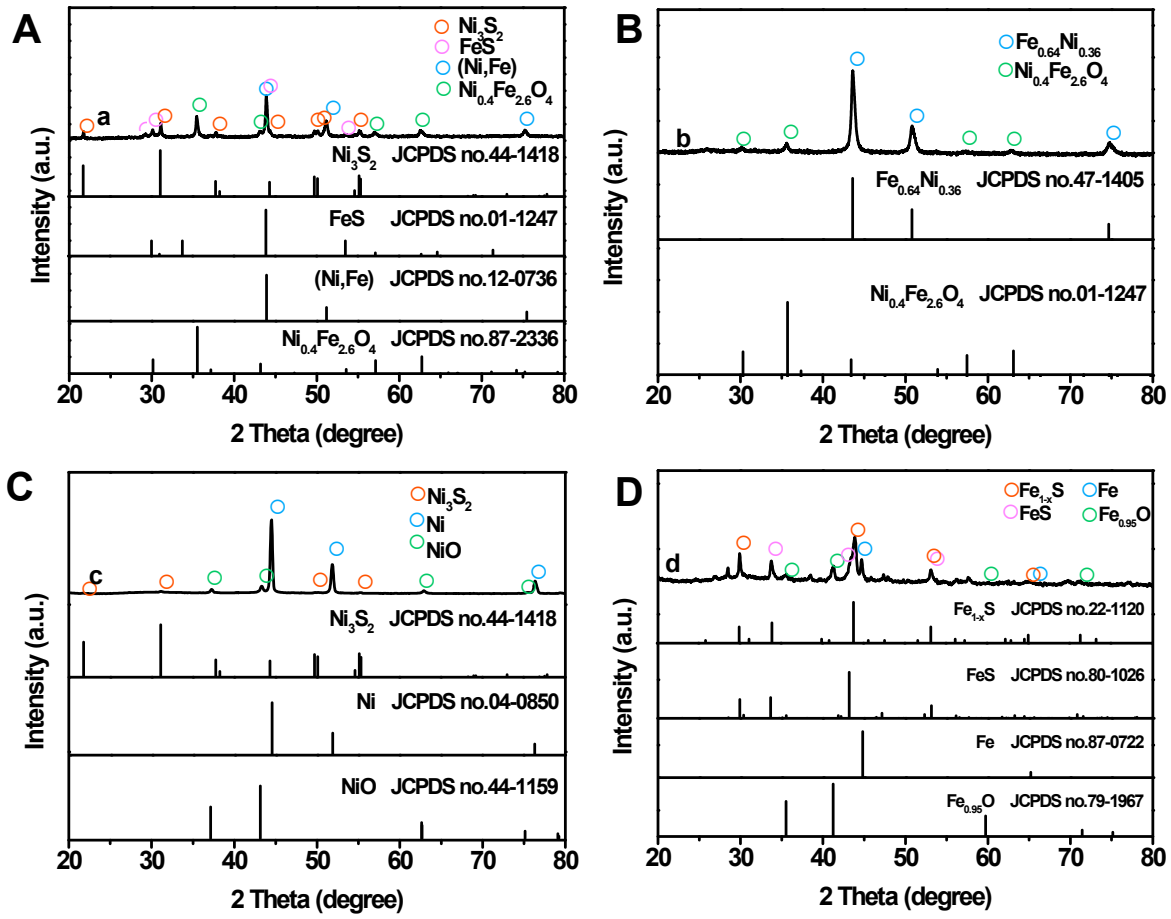

Fig. S8 XRD patterns of (a) 23-S-FeNi@NC-3, (b) FeNi@NC-3, (c) 23-S-Ni@NC-3 and (d) 23-S-Fe@NC-3. Noting, FeS was identified according to JCPDS no. 01-1247 and 23-1123.

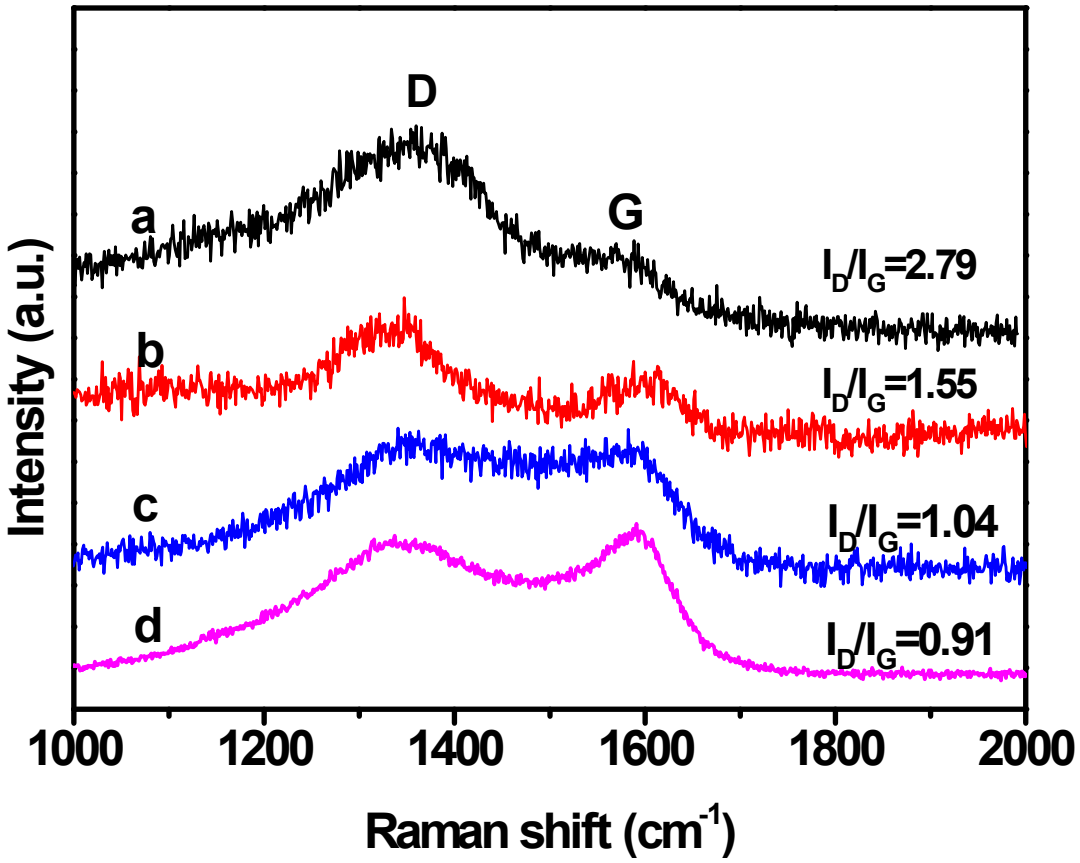

Fig. S9 Raman spectra of (a) 23-S-FeNi@NC-3, (b) FeNi@NC-3, (c) 23-S-Ni@NC-3 and (d) 23-S-Fe@NC-3.

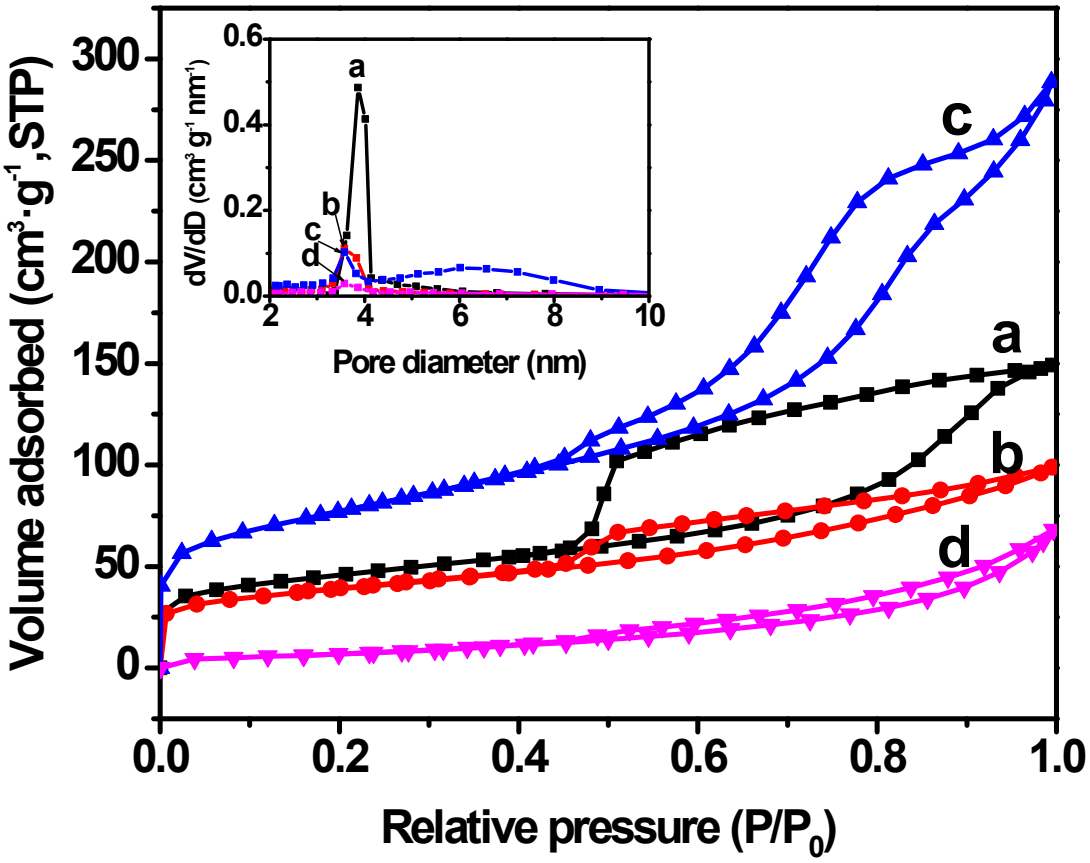

Fig. S10 Nitrogen absorption/desorption isotherm and the corresponding pore size distribution of (a) 23-S-FeNi@NC-3, (b) FeNi@NC-3, (c) 23-S-Ni@NC-3 and (d) 23-S-Fe@NC-3.

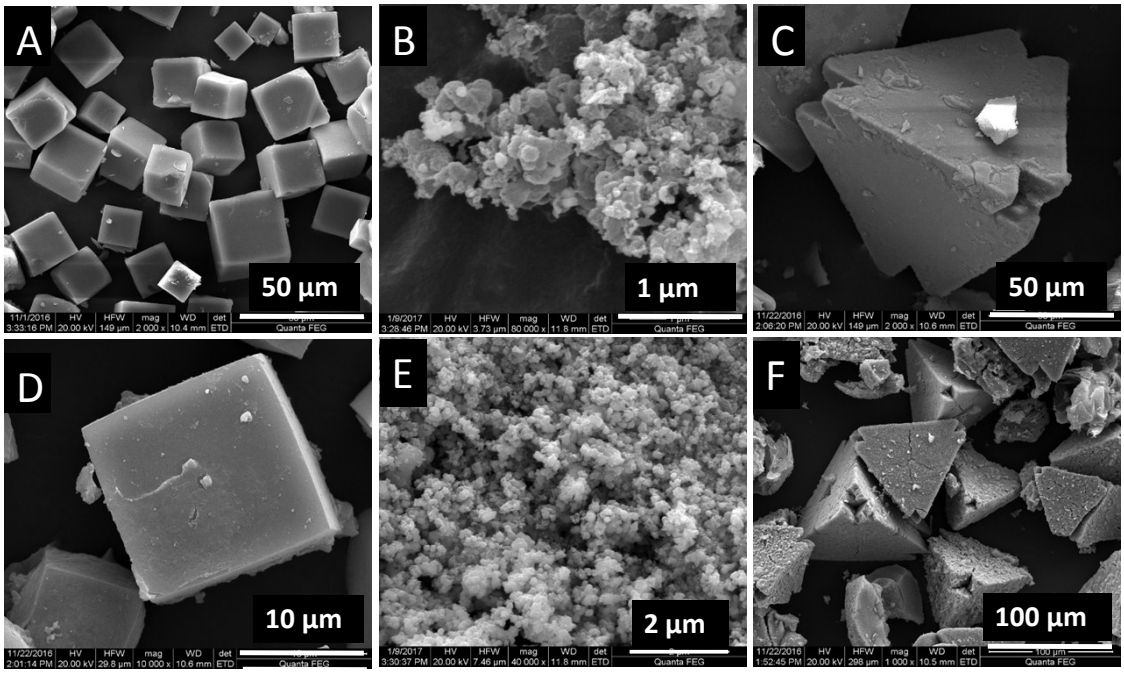

Fig. S11 SEM images of (A) FeNi-, (B) 23-S@Ni-, (C) 23-S@Fe-coordinated precursors, and their derived- (D) FeNi@NC-3, (E) 23-S-Ni@NC-3 and (F) 23-S-Fe@NC-3.

Table S4. Electrochemical Parameters of S-FeNi-Based catalysts

catalysts	η^{20} (mV)	Tafel slop (mV dec^{-1})	C_{dl} (mF cm^{-2})	R_{ct} (Ω cm^2)	R_{p1} (Ω cm^2)	TOF (10^{-2} s^{-1})	
						300 mV	400 mV
FeNi@NC-3	294	92	3.00	2.30	0.24	4.44	28.4
23-S-Ni@NC-3	377	139	2.99	8.84	0.18	1.57	7.5
23-S-Fe@NC-3	399	106	2.90	45.63	0.59	1.98	0.49
23-S-FeNi@NC-3	272	84	3.52	1.80	0.44	8.45	42.6
23-S-FeNi@NC-2	314	86	2.34				
23-S-FeNi@NC-4	328	94	3.00				

Table S5. Comparison of OER activities for reported Catalysts

Catalysts	Electrolyte	Catalyst loading (mg cm^{-2})	η^{20} (mV)	Tafel slop (mV dec^{-1})	Ref.
23-S-FeNi@NC-3	1.0 M KOH	0.14	272	84	This work
Fe/Ni-BTC@NF	0.1 M KOH	-	296	47	1
Ni_3S_2/NF	1.0 M KOH	1.60	289	-	2
FeNi/$NiFe_2O4$@NC-800	1.0 M KOH	0.14	336	60	3
S-NiFe-700@C	1.0 M KOH	0.286	297	53	4
Co_3O_4@C-MWCNTs	1.0 M KOH	0.325	346	62	5
Co-P/NC	1.0 M KOH	0.283	380	52	6
CoP/rGO-400	1.0 M KOH	0.28	383	66	7
Co_3O_4 microframes	1.0 M KOH	0.286	386	53	8
NiCo-UMOFNs	1.0 M KOH	0.2	263	42	9
Co_3O_4/$NiCo_2O_4$ DSNCs	1.0 M KOH	1.0	368	88	10
Activated Mn-Co oxide	1.0 M KOH	0.25	335	52	11
1.0%Ag-$CoSe_2$	0.1 M KOH	0.20	348	56	12
NCNT/CoO-NiO-NiCo	1.0 M KOH	0.21	299	40	13
FeCoW oxy-hydroxide	1.0 M KOH	0.24	205	-	14
$NixFe_{1-x}Se_2$	1.0 M KOH	-	201	28	15
NF@NC-$CoFe_2O_4$/C NRAs	1.0 M KOH	1.03	262	45	16
NPCN/CoNi-NCNT	0.1 M KOH	0.510	389	165	17
m-FeNi@NC	0.1 M KOH	0.510	426	59.1	18
Plasma-engraved Co_3O_4 nanosheets	0.1 M KOH	−	323	68	19
NiCo LDH	1.0 M KOH	0.17	393	40	20

Table S6. Circuit modeling, R(C(R(Q(R(CR))))), results of S-FeNi@NC with ZSimpWin simulating programme

Catalyst / Circuit Components	23-S-FeNi@NC-3		FeNi@NC-3		23-S-Ni@NC-3		23-S-Fe@NC-3	
	Fitted value	Error, %	Fitted value	Error, %	Fitted value	Error, %	Fitted value	Error,%
R_s (Ω cm^2)	0.61	7.39	0.61	2.90	0.56	4.01	0.44	17.61
C_p (μF cm^{-2})	3.60	21.52	21.69	18.75	10.38	25.97	0.73	2.81
R_{p1} (Ω cm^2)	0.44	9.93	0.24	7.40	0.18	11.49	0.59	14.37
Q (mS s-n cm^{-2})	12.22	6.28	6.62	19.23	13.28	4.42	3.524	7.30
n	0.85	1.44	0.75	3.89	0.77	0.94	0.711	2.52
R_{p2} (Ω cm^2)	0.012	168	0.69	12.10	9.21	7.68	0.73	2.52
C_{dl} (mF cm^{-2})	0.20	1.93	2.64	11.42	7.10	11.60	1.44	8.40
R_{ct} (Ω cm^2)	1.80	9.86	2.30	4.09	8.84	7.24	45.63	5.55
x^2	7.57×10^{-4}		1.99×10^{-3}		5.95×10^{-4}		3.24×10^{-3}	

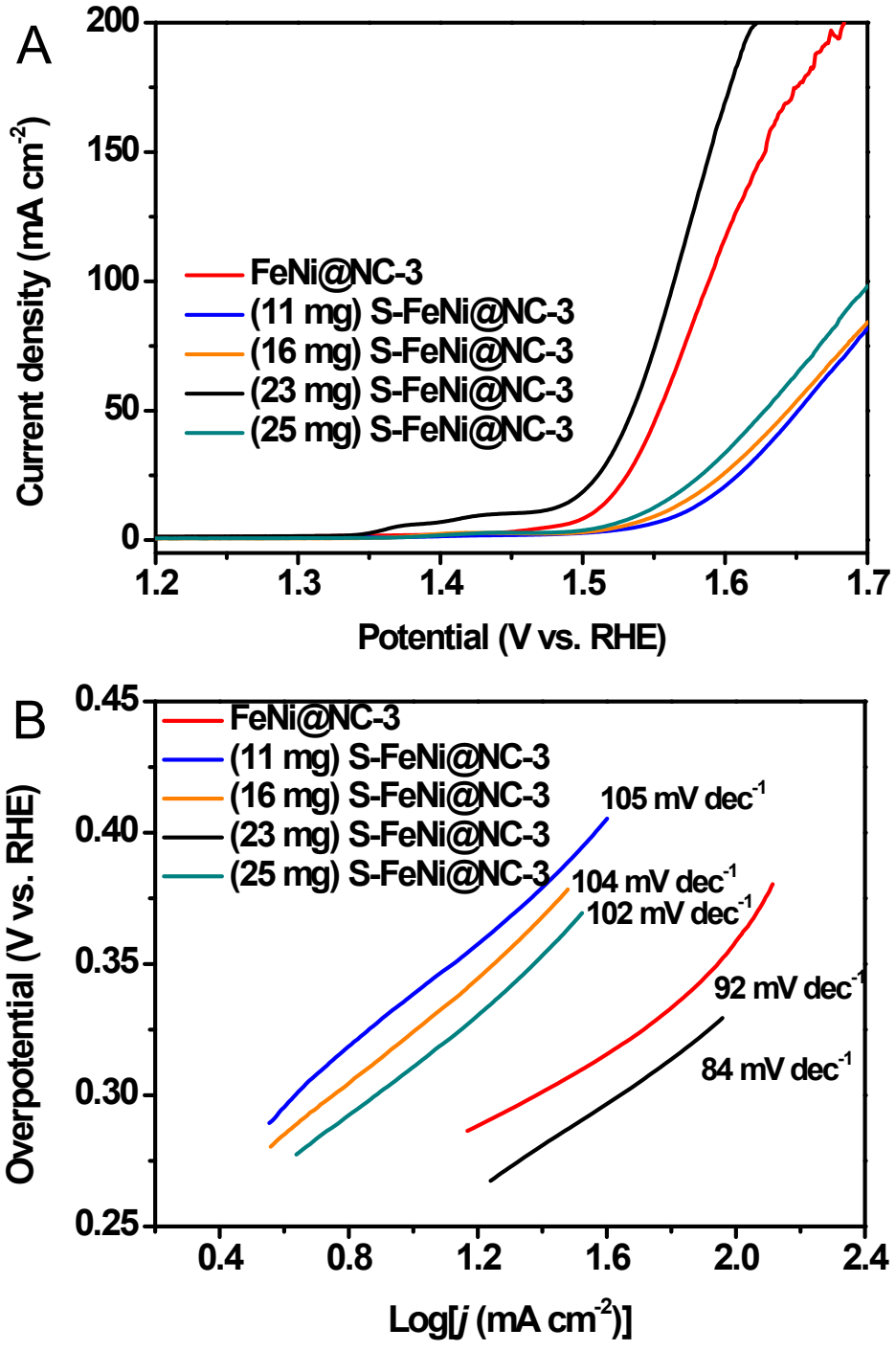

Fig. S12 (A) LSV curves, (B) Tafel plots of S-Fe@NC-3 with various amount of sulfur.

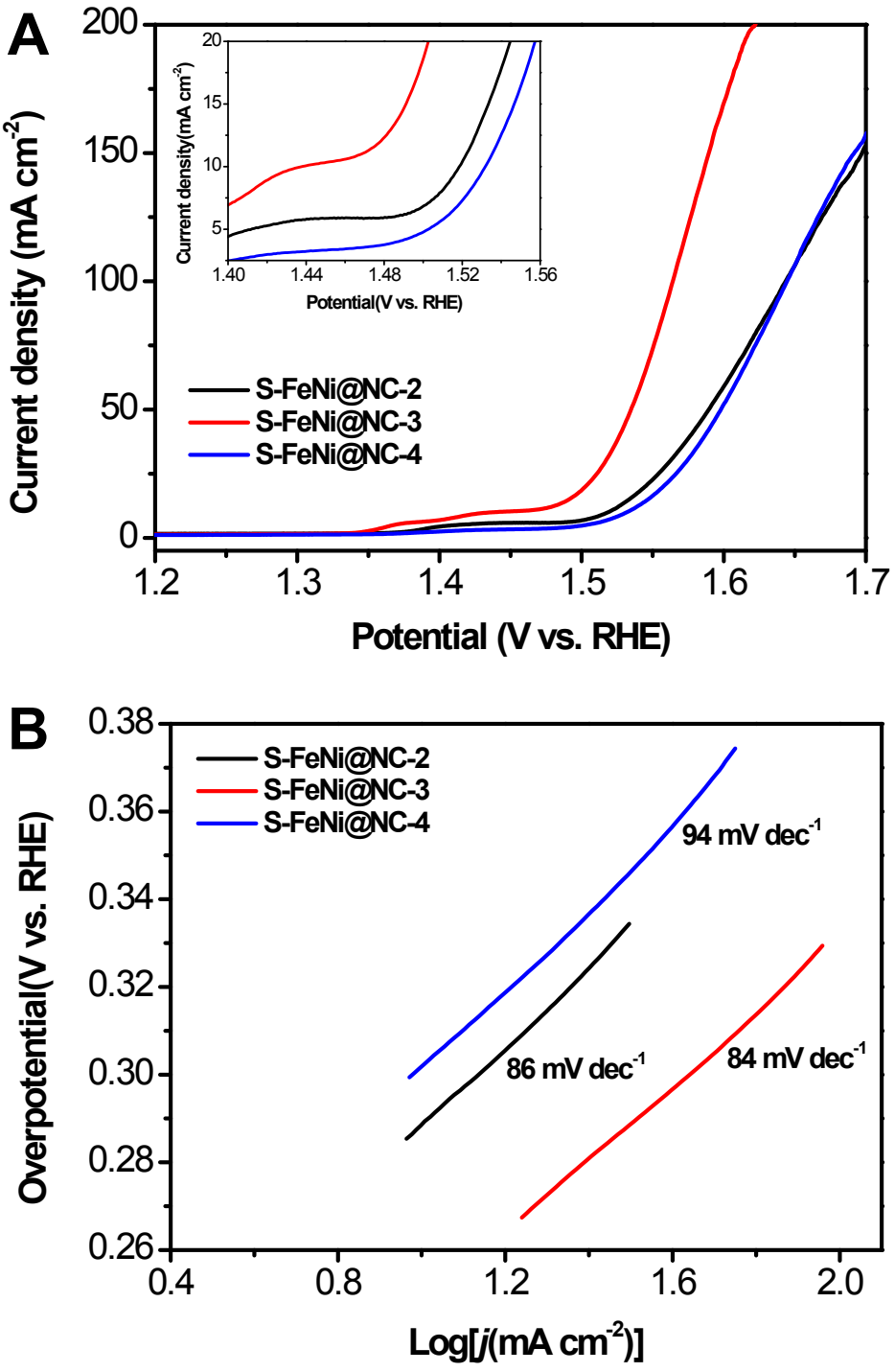

Fig. S13 (A) LSV curves, (B) Tafel plots in 1.0 M KOH of 23-S-FeNi@NC-2, 23-S-FeNi@NC-3 and 23-S-FeNi@NC-4.

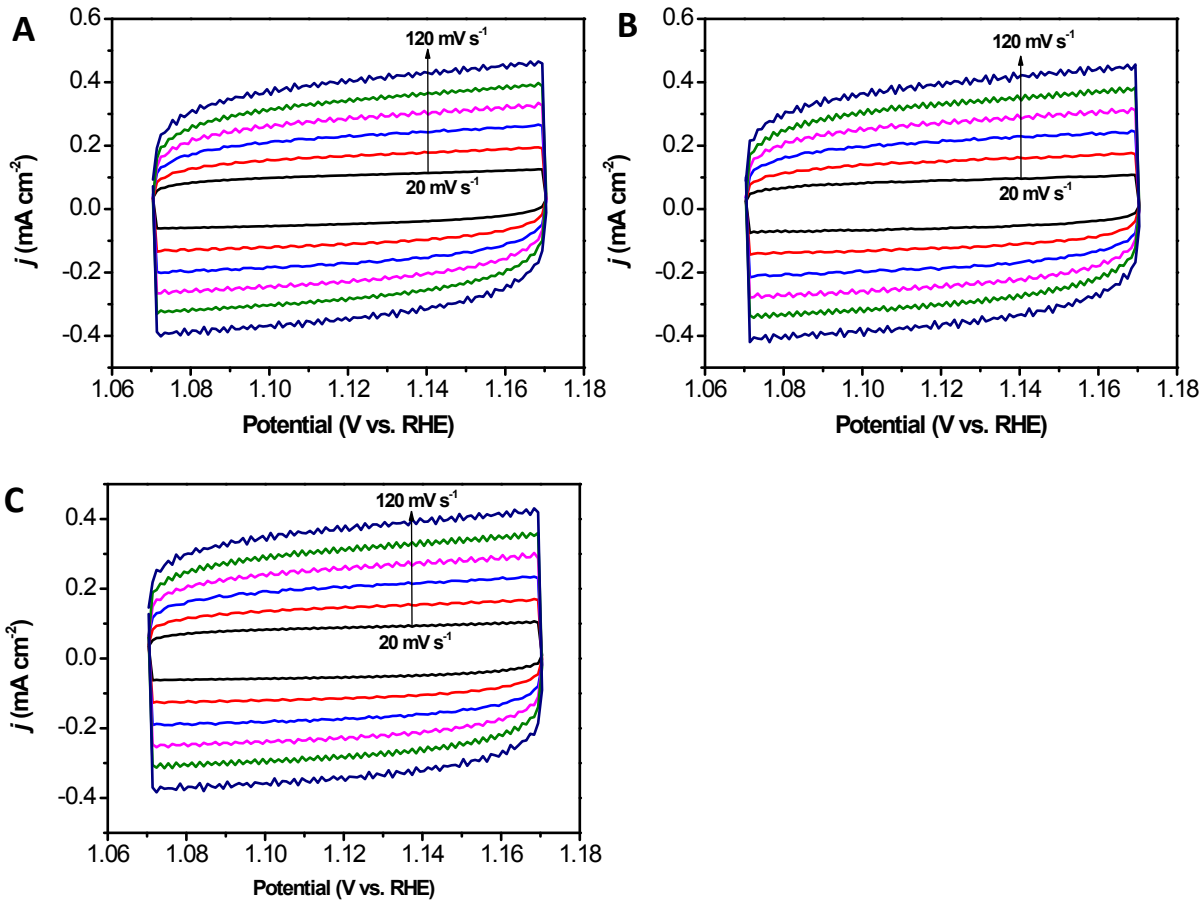

Fig. S14 Cyclic voltammograms (1.07–1.17 V vs. RHE) of (A) FeNi@NC-3, (B) 23-S-Ni@NC-3 and (C) 23-S-Fe@NC-3 in 1.0 M KOH at scan rates of 20 to 120 mV.

REFERENCES

1 L. Wang, Y. Wu, R. Cao, L. Ren, M. Chen, X. Feng, J. Zhou, B. Wang, *ACS Appl. Mater. Inter.* 2016, **8**, 16736.

2 L. L. Feng, G. Yu, Y. Wu, G. D. Li, H. Li, Y. Sun, T. Asefa, W. Chen, X. Zou, *J. Am. Chem. Soc.* 2015, **137**, 14023.

3 Y. D. Ma, X. P. Dai, M. Z. Liu, J. X. Yong, H. Y. Qiao, A. X. Jin, Z. Z. Li, X. L. Huang, H. Wang, X. Zhang, *ACS Appl. Mater. Inter.* 2016, **8**, 34396-34404.

4 Y. Feng, X. Yu, U. Paik, *Sci. Rep.* 2016, **6**, 34004.

5 X. Li, Y. Fang, X. Lin, M. Tian, X. An, Y. Fu, R. Li, J. Jin, J. Ma, *J. Mater. Chem. A* 2015, **3**, 17392.

6 B. You, N. Jiang, M. Sheng, S. Gul, J. Yano, Y. Sun, *Chem. Mater.* 2015, **27**, 7636.

7 L. Jiao, Y. Zhou, H. Jiang, *Chem. Sci.* 2016, **7**, 1690.

8 Y. Feng, X. Yu, U. Paik, *Chem. Commun.* 2016, **52**, 6269.

9 S. Zhao, Y. Wang, J. Dong, C. He, H. Yin, P. An, K. Zhao, X. Zhang, C. Gao, L. Zhang, J. Lv, J. Wang, J. Zhang, A. Khattak, N. Khan, Z. Wei, J. Zhang, S. Liu, H. Zhao, Z. Tang, *Nature Energy* 2016, **1**, 16184.

10 H. Hu, B. Guan, B. Xia, X. W. Lou, *J. Am. Chem. Soc.* 2015, **137**, 5590.

11 B. Guan, L. Yu, X. Lou, *Angew. Chem. Int. Ed.* 2017, **56**, 2386-2389.

12 X. Zhao, H. Zhang, Y. Yan, J. Cao, S. Zhou, X. Li, Z. Peng, J. Zeng, *Angew. Chem. Int. Ed.* 2017, **56**, 328.

13 X. Liu, M. Park, M. Kim, S. Gupta, G. Wu, J. Cho, *Angew. Chem. Int. Ed.* 2015, **54**, 9654.

14 B. Zhang, X. Zheng, O. Voznyy, R. Comin, M. Bajdich, M. García-Melchor, L. Han, J. Xu, M. Liu, L. Zheng, et al., *Science* 2016, **352**, 333.

15 X. Xu, F. Song, X. Hu, *Nat. Commun.* 2016, **7**, 12324.

16 X. Lu, L. Gu, J. Wang, J. Wu, P. Liao, G. Li, *Adv. Mater.* 2017, **29**, 1604437.

17 Y. Hou, S. Cui, Z. Wen, X. Guo, X. Feng, J. Chen, *Small* 2015, **11**, 5940.

18 S. Ci, S. Mao, Y. Hou, S. Cui, H. Kim, R. Ren, Z. Wen, J. Chen, *J. Mater. Chem. A* 2015, **3**, 7986.

19 L. Xu, Q. Jiang, Z. Xiao, X. Li, J. Huo, S. Wang, L. Dai, *Angew. Chem. Int. Ed.* 2016, **55**, 5277.

20 H. Liang, F. Meng, M. Cabán-Acevedo, L. Li, A. Forticaux, L. Xiu, Z. Wang, S. Jin, *Nano lett.* 2015, **15**, 1421.